Drug-microenvironment perturbations reveal resistance mechanisms and prognostic subgroups in CLL

Appendix

Peter-Martin Bruch*, Holly A. R. Giles*, Carolin Kolb , Sophie A. Herbst, Tina Becirovic, Tobias Roider, Junyan Lu, Sebastian Scheinost, Lena Wagner, Jennifer Huellein, Ivan Berest, Mark Kriegsmann, Katharina Kriegsmann, Christiane Zgorzelski, Peter Dreger, Judith B. Zaugg, Carsten Müller-Tidow, Thorsten Zenz, Wolfgang Huber*, Sascha Dietrich* * These authors contributed equally to this work.

14th April 2022

Contents

Appendix Tables

Patient ID	Sex	Treated before	IGHV status	Methylation Cluster	Del(13q)	Del(11q)	Trisomy 12	Del(17p)
Pat_001	female	Yes	unmutated	Low Programmed	1	0	0	0
Pat_002	male	Yes	mutated	Intermediate Programmed	1	0	0	0
Pat_003	male	No	mutated	High Programmed	0	0	1	0
Pat_004	female	Yes	unmutated	Low Programmed	0	1	0	0
Pat_005	male	No	unmutated	Low Programmed	1	0	0	0
Pat_006	female	No	unmutated	Low Programmed	0	0	0	0
Pat_007	female	No	mutated	High Programmed	1	0	0	0
Pat_008	male	Yes	unmutated	Low Programmed	1	0	0	0
Pat_009	male	Yes	unmutated	Low Programmed	1	0	0	1
Pat_010	female	Yes	unmutated	Low Programmed	1	0	0	1
Pat_011	female	No	unmutated	NA	0	0	1	0
Pat_012	female	No	mutated	High Programmed	1	0	0	0
Pat_013	female	Yes	unmutated	Intermediate Programmed	1	1	0	0
Pat_014	male	No	mutated	High Programmed	0	0	0	0
Pat_015	male	No	mutated	High Programmed	1	0	0	0
Pat_016	male	No	mutated	High Programmed	1	0	0	0
Pat_017	male	No	mutated	NA	1	0	0	0
Pat_018	female	Yes	unmutated	Low Programmed	1	1	0	0
Pat_019	male	No	mutated	High Programmed	1	0	0	0
Pat_020	female	Yes	mutated	Intermediate Programmed	1	0	0	0
Pat_021	male	No	unmutated	Low Programmed	0	0	0	1
Pat_022	female	No	mutated	Intermediate Programmed	0	0	1	0
Pat_023	female	No	mutated	High Programmed	0	0	0	0
Pat_024	female	Yes	mutated	High Programmed	0	0	0	1
Pat_025	male	No	mutated	Intermediate Programmed	1	0	0	0
Pat_026	male	No	mutated	High Programmed	1	0	0	0
Pat_027	female	No	mutated	High Programmed	1	0	0	0
Pat_028	female	No	mutated	Intermediate Programmed	1	0	0	0
Pat_029	female	No	mutated	High Programmed	1	0	0	0
Pat_030	male	Yes	mutated	High Programmed	1	0	0	0
Pat_031	male	No	mutated	High Programmed	0	0	0	0
Pat_032	female	Yes	unmutated	Low Programmed	1	1	0	0
Pat_033	male	Yes	unmutated	Intermediate Programmed	0	1	0	0
Pat_034	male	Yes	unmutated	Low Programmed	0	1	0	0
Pat_035	male	No	mutated	High Programmed	1	0	0	0
Pat_036	male	Yes	unmutated	Low Programmed	1	1	0	1
Pat_037	female	Yes	unmutated	Intermediate Programmed	1	0	0	0
Pat_038	male	No	mutated	Intermediate Programmed	1	0	0	0
Pat_039	male	Yes	mutated	High Programmed	1	0	0	0
Pat_040	female	No	mutated	High Programmed	0	0	0	0
Pat_041	female	Yes	unmutated	Low Programmed	0	0	1	0
Pat_042	female	No	mutated	Intermediate Programmed	1	1	0	0
Pat_043	female	No	mutated	High Programmed	1	0	0	0
Pat_044	male	No	mutated	High Programmed	1	0	0	0
Pat_045	male	No	unmutated	Low Programmed	0	0	0	0
Pat_046	male	No	mutated	Intermediate Programmed	0	0	1	0
Pat_047	male	No	mutated	High Programmed	1	0	0	0
Pat_048	male	No	mutated	High Programmed	1	0	0	0
Pat_049	female	No	mutated	Intermediate Programmed	0	1	0	0
Pat_050	male	No	mutated	High Programmed	0	0	1	0
Pat_051	male	No	mutated	NA	1	0	0	0
Pat_052	female	No	mutated	Intermediate Programmed	1	0	0	0
Pat_053	male	Yes	unmutated	Low Programmed	1	1	0	0
Pat_054	female	Yes	unmutated	Low Programmed	0	1	0	0
Pat_055	male	Yes	unmutated	Low Programmed	0	0	0	0
Pat_056	female	No	unmutated	Low Programmed	NA	NA	NA	NA
Pat_057	female	No	mutated	High Programmed	1	0	1	0
Pat_058	female	Yes	unmutated	Low Programmed	0	0	0	0

(continued)

Patient ID	Sex	Treated before	IGHV status	Methylation Cluster	Del(13q)	Del(11q)	Trisomy 12	Del(17p)
Pat_059	male	No	mutated	High Programmed	1	0	0	0
Pat_060	male	Yes	mutated	Intermediate Programmed	1	0	0	1
Pat_061	male	No	unmutated	Low Programmed	0	0	1	0
Pat_062	male	Yes	unmutated	Low Programmed	1	1	0	0
Pat_063	female	No	unmutated	Low Programmed	1	0	0	0
Pat_064	male	Yes	unmutated	Low Programmed	1	1	0	1
Pat_065	male	No	unmutated	Low Programmed	0	1	0	0
Pat_066	male	Yes	unmutated	Low Programmed	1	1	0	0
Pat_067	female	No	mutated	High Programmed	1	0	0	0
Pat_068	male	No	mutated	High Programmed	1	0	0	0
Pat_069	male	Yes	mutated	High Programmed	1	0	0	0
Pat_070	female	No	mutated	High Programmed	0	0	0	0
Pat_071	female	No	unmutated	Low Programmed	0	0	0	0
Pat_072	male	Yes	mutated	High Programmed	0	0	1	0
Pat_073	female	No	unmutated	Low Programmed	1	1	0	0
Pat_074	female	No	mutated	High Programmed	0	0	0	0
Pat_075	female	No	mutated	High Programmed	1	0	0	0
Pat_076	male	No	mutated	High Programmed	1	0	0	0
Pat_077	female	No	unmutated	NA	0	0	1	0
Pat_078	male	No	unmutated	Low Programmed	0	0	0	0
Pat_079	male	No	mutated	High Programmed	1	0	0	0
Pat_080	female	No	mutated	High Programmed	0	0	0	0
Pat_081	male	No	mutated	High Programmed	0	0	0	0
Pat_082	male	No	unmutated	Low Programmed	0	0	0	0
Pat_083	male	No	mutated	High Programmed	0	0	0	0
Pat_084	male	No	unmutated	Low Programmed	0	0	1	0
Pat_085	male	No	mutated	High Programmed	0	0	0	0
Pat_086	male	Yes	unmutated	Low Programmed	1	1	0	0
Pat_087	male	No	mutated	Intermediate Programmed	1	0	0	0
Pat_088	female	Yes	unmutated	Low Programmed	1	0	0	1
Pat_089	male	No	mutated	High Programmed	0	0	0	0
Pat_090	male	Yes	unmutated	Low Programmed	0	0	1	0
Pat_091	male	Yes	mutated	NA	1	0	0	0
Pat_092	male	Yes	mutated	High Programmed	0	0	0	0
Pat_093	male	No	mutated	High Programmed	1	0	0	0
Pat_094	female	Yes	mutated	High Programmed	0	0	0	0
Pat_095	male	Yes	unmutated	Low Programmed	0	0	0	0
Pat_096	male	No	mutated	High Programmed	0	0	0	0
Pat_097	female	Yes	unmutated	Low Programmed	0	0	0	0
Pat_098	male	No	mutated	High Programmed	1	0	0	0
Pat_099	female	No	unmutated	Low Programmed	1	0	0	0
Pat_100	female	No	unmutated	Low Programmed	1	0	0	0
Pat_101	female	No	unmutated	Low Programmed	1	0	0	0
Pat_102	male	Yes	unmutated	Intermediate Programmed	0	0	0	0
Pat_103	female	No	mutated	High Programmed	1	0	1	0
Pat_104	female	Yes	mutated	High Programmed	0	0	0	0
Pat_105	male	No	unmutated	Low Programmed	NA	NA	NA	NA
Pat_106	male	No	unmutated	Low Programmed	1	1	0	1
Pat_107	female	No	mutated	NA	1	0	0	0
Pat_108	male	No	mutated	NA	1	0	1	0
Pat_109	male	No	mutated	High Programmed	1	0	0	0
Pat_110	male	No	mutated	Intermediate Programmed	1	1	0	0
Pat_111	female	Yes	unmutated	Low Programmed	1	0	0	0
Pat_112	female	No	mutated	NA	0	0	1	0
Pat_113	female	No	mutated	High Programmed	1	0	0	0
Pat_114	male	No	unmutated	Low Programmed	1	0	0	0
Pat_115	male	Yes	unmutated	Low Programmed	1	0	0	1
Pat_116	male	No	unmutated	Low Programmed	1	0	0	0
Pat_117	male	No	unmutated	Intermediate Programmed	1	0	0	0
Pat_118	female	No	mutated	High Programmed	0	0	0	1

(continued)

Patient ID	Sex	Treated before	IGHV status	Methylation Cluster	Del(13q)	Del(11q)	Trisomy 12	Del(17p)
Pat_119	male	No	unmutated	Low Programmed	NA	NA	NA	NA
Pat_120	female	No	unmutated	Low Programmed	0	0	1	0
Pat_121	male	No	unmutated	Low Programmed	0	0	0	1
Pat_122	male	No	unmutated	Low Programmed	0	1	0	0
Pat_123	male	No	unmutated	Low Programmed	1	0	0	1
Pat_124	female	No	mutated	High Programmed	1	0	1	0
Pat_125	female	No	mutated	High Programmed	1	0	0	0
Pat_126	male	Yes	NA	NA	0	0	1	0
Pat_127	male	No	unmutated	Low Programmed	1	1	0	1
Pat_128	male	No	mutated	High Programmed	1	0	0	0
Pat_129	male	Yes	unmutated	Low Programmed	1	0	0	0
Pat_130	female	No	mutated	Intermediate Programmed	1	0	0	0
Pat_131	female	No	unmutated	Low Programmed	1	0	0	1
Pat_132	male	Yes	unmutated	Low Programmed	1	0	0	1
Pat_133	male	Yes	unmutated	Low Programmed	1	0	0	1
Pat_134	male	Yes	mutated	High Programmed	1	0	0	1
Pat_135	male	No	mutated	High Programmed	1	0	0	0
Pat_136	male	No	mutated	High Programmed	1	0	0	0
Pat_137	female	No	unmutated	Low Programmed	0	0	1	0
Pat_138	female	No	mutated	High Programmed	1	0	0	0
Pat_139	female	No	mutated	High Programmed	NA	NA	NA	NA
Pat_140	female	No	mutated	Intermediate Programmed	1	0	0	0
Pat_141	male	No	mutated	Intermediate Programmed	1	0	0	0
Pat_142	male	No	mutated	High Programmed	1	0	0	0
Pat_143	female	No	unmutated	Low Programmed	1	0	0	0
Pat_144	male	Yes	unmutated	Low Programmed	0	0	0	1
Pat_145	female	No	mutated	High Programmed	0	0	0	0
Pat_146	male	Yes	unmutated	Low Programmed	NA	NA	NA	NA
Pat_147	male	Yes	unmutated	Low Programmed	0	0	0	1
Pat_148	male	Yes	unmutated	NA	1	0	0	0
Pat_149	male	Yes	unmutated	Low Programmed	0	1	1	0
Pat_150	female	No	mutated	High Programmed	1	0	0	NA
Pat_151	male	No	unmutated	Low Programmed	0	0	1	0
Pat_152	male	No	NA	NA	0	1	1	0
Pat_153	male	Yes	unmutated	Low Programmed	1	0	0	0
Pat_154	male	No	mutated	High Programmed	1	0	0	0
Pat_155	male	No	mutated	High Programmed	1	0	0	0
Pat_156	female	No	unmutated	Low Programmed	1	0	0	0
Pat_157	female	No	unmutated	Low Programmed	1	1	0	0
Pat_158	male	No	mutated	High Programmed	1	0	0	0
Pat_159	female	No	unmutated	Low Programmed	1	0	0	0
Pat_160	male	No	unmutated	Low Programmed	NA	NA	NA	NA
Pat_161	male	Yes	unmutated	Low Programmed	0	0	0	0
Pat_162	male	No	mutated	High Programmed	0	0	0	0
Pat_163	male	No	mutated	High Programmed	0	0	0	0
Pat_164	female	No	unmutated	Low Programmed	0	0	0	0
Pat_165	male	Yes	unmutated	Low Programmed	0	1	1	0
Pat_166	male	No	unmutated	Low Programmed	1	0	1	0
Pat_167	male	No	NA	Intermediate Programmed	NA	NA	NA	NA
Pat_168	male	No	mutated	High Programmed	1	1	0	0
Pat_169	male	No	mutated	High Programmed	0	0	1	0
Pat_170	male	No	mutated	High Programmed	1	0	0	0
Pat_171	male	No	mutated	High Programmed	1	0	0	0
Pat_172	male	No	mutated	High Programmed	1	0	0	0
Pat_173	male	No	mutated	High Programmed	1	0	0	0
Pat_174	female	No	unmutated	Low Programmed	NA	0	NA	0
Pat_175	male	No	unmutated	Low Programmed	0	0	0	0
Pat_176	female	No	mutated	High Programmed	NA	NA	NA	NA
Pat_177	female	No	NA	Intermediate Programmed	NA	1	NA	NA
Pat_178	male	No	mutated	High Programmed	1	0	0	0

(continued)

Patient ID	Sex	Treated before	IGHV status	Methylation Cluster	Del(13q)	Del(11q)	Trisomy 12	Del(17p)
Pat_179	male	No	unmutated	Low Programmed	0	1	0	0
Pat_180	male	No	mutated	High Programmed	NA	NA	NA	NA
Pat_181	female	No	mutated	High Programmed	NA	NA	NA	NA
Pat_182	male	No	mutated	High Programmed	1	0	0	0
Pat_183	female	Yes	NA	Intermediate Programmed	1	0	0	0
Pat_184	male	No	unmutated	Low Programmed	NA	NA	NA	NA
Pat_185	male	No	mutated	High Programmed	NA	NA	NA	NA
Pat_186	male	No	mutated	High Programmed	1	0	0	0
Pat_187	male	Yes	unmutated	Low Programmed	NA	NA	NA	NA
Pat_188	male	No	NA	NA	NA	NA	NA	NA
Pat_189	male	No	NA	NA	NA	NA	NA	NA
Pat_190	male	No	NA	NA	NA	NA	NA	NA
Pat_191	female	No	NA	NA	0	0	0	0
Pat_192	female	No	NA	NA	1	0	0	0

Appendix Table 1. Patient samples included in the study.

List of patient samples and selected characteristics. For a full list of characteristics see online vignette.NA=Not available.

Genetic feature	Wildtype/IGHV unmutated	Mutated/ IGHV Mutated	Not available
ATM	164	16	12
BIRC3	177	3	12
CARD11	135	3	54
Complex_Karyotype	115	31	46
CREBBP	135	3	54
CSMD3	175	5	12
del11p	143	3	46
del11q	148	28	16
del12q	171	3	18
del13q	66	108	18
del14q	145	5	42
del15q	141	5	46
del17p	154	20	18
del17q	143	3	46
del18p	141	5	46
del1q	141	5	46
del21q	143	3	46
del3p	143	3	46
del3q	143	3	46
del4p	143	3	46
del4q	143	3	46
del6q	166	7	19
del7q	143	3	46
del8p	135	11	46
del9p	140	6	46
del9q	142	4	46
EGR2	176	4	12
FAT2	175	5	12
FAT4	176	4	12
FBXW7	178	3	11
FLRT2	135	3	54
gain17q	143	3	46
gain18q	144	4	44
gain19p	142	4	46
gain19q	142	4	46
gain1q	143	3	46
gain2p	137	9	46
gain8q	159	13	20
IGHV.status	83	99	10
IKZF3	176	4	12
MED12	170	10	12
MYD88	184	3	5
NFKBIE	175	5	12
NOTCH1	137	24	31
POT1	174	6	12
Ras_Raf	170	15	7
RYR2	177	3	12
SF3B1	161	26	5
SPEN	177	3	12
TP53	157	30	5
trisomy12	149	25	18
U1	137	5	50
XPO1	175	5	12
ZMYM3	134	4	54

Appendix Table 2. List of genetic features tested for their association with stimulus response in the univariate model of Figure 3A.

Only genetic features with at least three positive cases were considered.

Factor	Hazard Ratio	p-value	CI Low	CI High
Cluster 3 vs Cluster 1	1.27	0.37	0.75	2.16
Cluster 3 vs Cluster 2	2.06	0.03	1.07	3.93
Cluster 3 vs Cluster 4	0.35	0.01	0.17	0.73

Appendix Table 3. Survival analysis of microenvironmental response clusters comparing C3 to C1, C2 and C4.

Cox proportional hazards model of stimulus response clusters using time to next treatment and with C3 as reference.

Factor	Hazard Ratio	p-value	CI Low	CI High
Cluster 3 vs combined Clusters 1 and 2	1.42	0.17	0.86	2.36

Appendix Table 4. Survival analysis of microenvironmental response clusters comparing C3 to C1 and C2 combined.

Cox proportional hazards model of stimuli response clusters using TTT.

Factor	Hazard Ratio	p-value	CI Low	CI High
Cluster 3 vs Cluster 1	0.95	0.87	0.52	1.74
Cluster 3 vs Cluster 2	1.64	0.23	0.74	3.63
Cluster 3 vs Cluster 4	0.34	0.03	0.13	0.88
IGHV.status	1.95	0.32	0.53	7.20
trisomy 12	1.04	0.93	0.48	2.23
TP53	3.88	<0.0001	2.25	6.68
Methylation_ClusterIP	1.57	0.3	0.67	3.70
Methylation_ClusterLP	1.00	1	0.25	4.04
POT1	2.65	0.07	0.93	7.54

Appendix Table 5. Multivariate survival analysis of response clusters.

Multivariate Cox proportional hazards model of stimulus response clusters and genetic subgroups of disease progression using time to next treatment with C3 as reference.

	Pathway	Geneset Database	Geneset Size	Spi-B targets (/333)	p-value	adj. p-value
JAK STAT signaling pathway	JAK STAT signaling pathway	KEGG	155	8	0.005	0.099

Appendix Table 6. Over-representation tests of immune signalling pathways (and control pathways) amongst Spi-B gene targets, based on primary CLL ATACseq data.

	Pathway	Geneset Database	Geneset Size	Spi-B targets (/3253)	SPIB p-value	SPIB adj. p-value
BCR Signaling Pathway	BCR Signaling Pathway	KEGG	75	36	0.000	0.000
TLR Signaling Pathway	TLR Signaling Pathway	KEGG	102	40	0.000	0.001
Signaling by TGFbeta Receptor Complex	Signaling by TGFbeta Receptor Complex	Reactome	75	26	0.011	0.071
TCR Signaling Pathway	TCR Signaling Pathway	KEGG	108	35	0.011	0.071

Appendix Table 7. Over-representation tests of immune signalling pathways (and control pathways) amongst Spi-B gene targets, based on DLBCL ChIPseq data from Care et al. 2014[1].

Appendix Figures

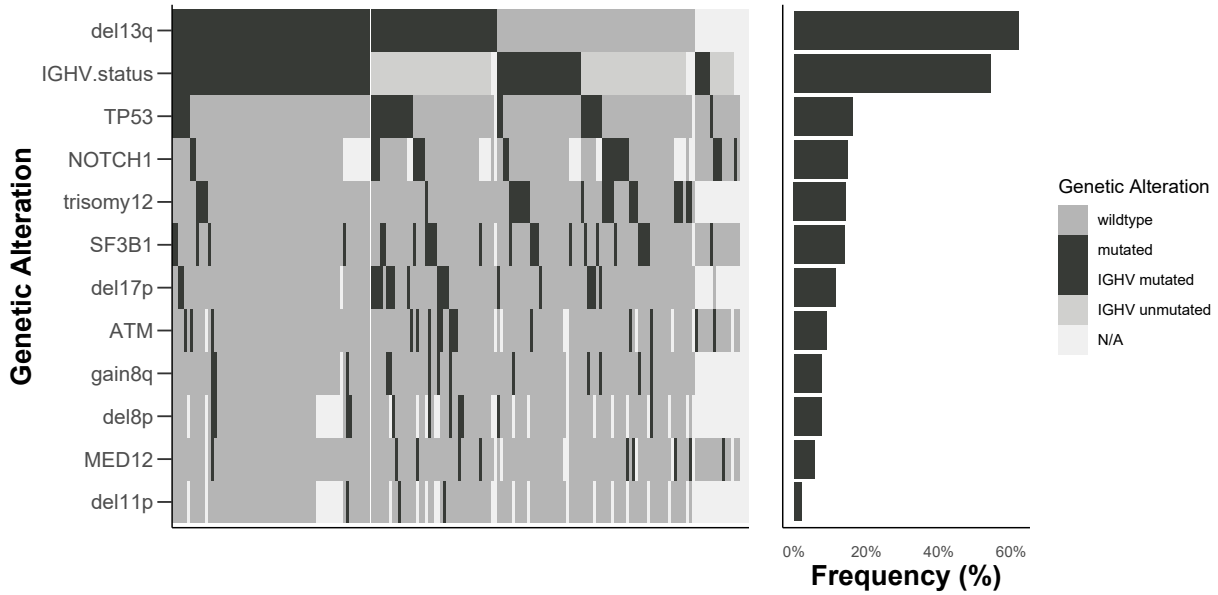

Appendix Figure 1. Genetic profiles of screened patient samples.

Selected genetic features on y-axis and patient samples (n=192) on x-axis.

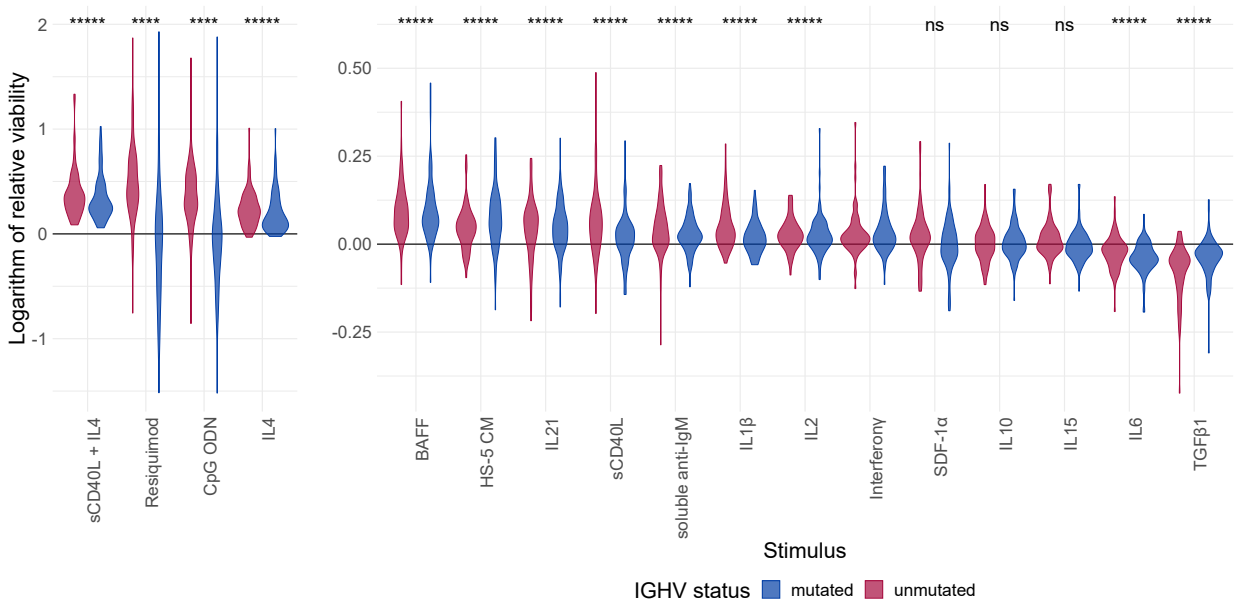

Appendix Figure 2. Response to stimuli stratified by IGHV status.

Logarithm of the relative viability after 48h incubation with microenvironmental stimuli, stratified by IGHV status (IGHV mutated: n=99; IGHV unmutated: n=83). BH-transformed p-values are shown from one-sample Student's t-tests of all patient samples. ($p<0.00001$=*****, $p<0.0001$=****, $p>0.05$=ns)

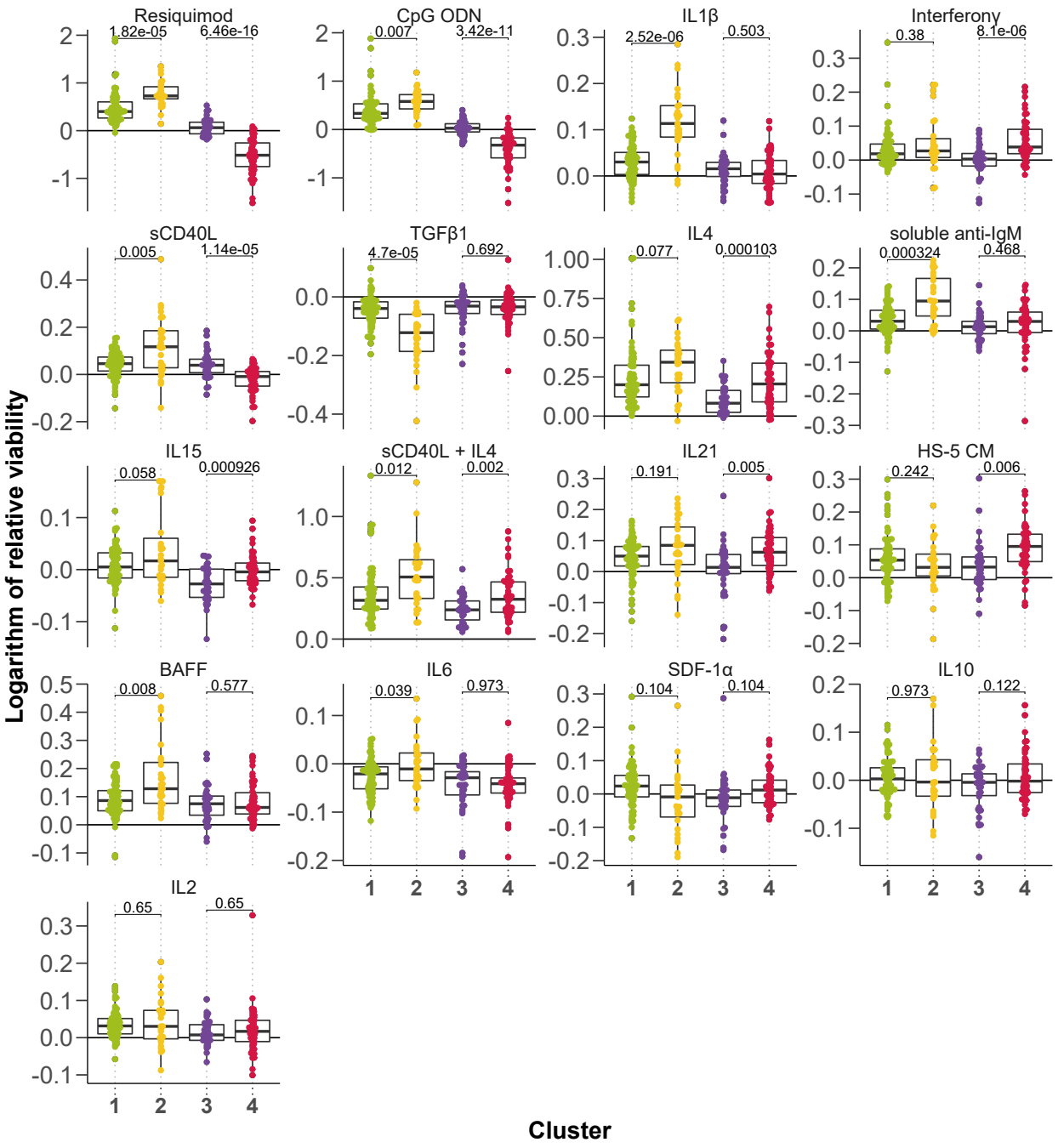

Appendix Figure 3. Stimulus response stratified by clusters.

Logarithm of the relative viability after treatment with stimuli, faceted by cluster. BH-transformed p-values from Student's t-test (C1: n=77; C2:n=27; C3: n=38; C4: n=50).

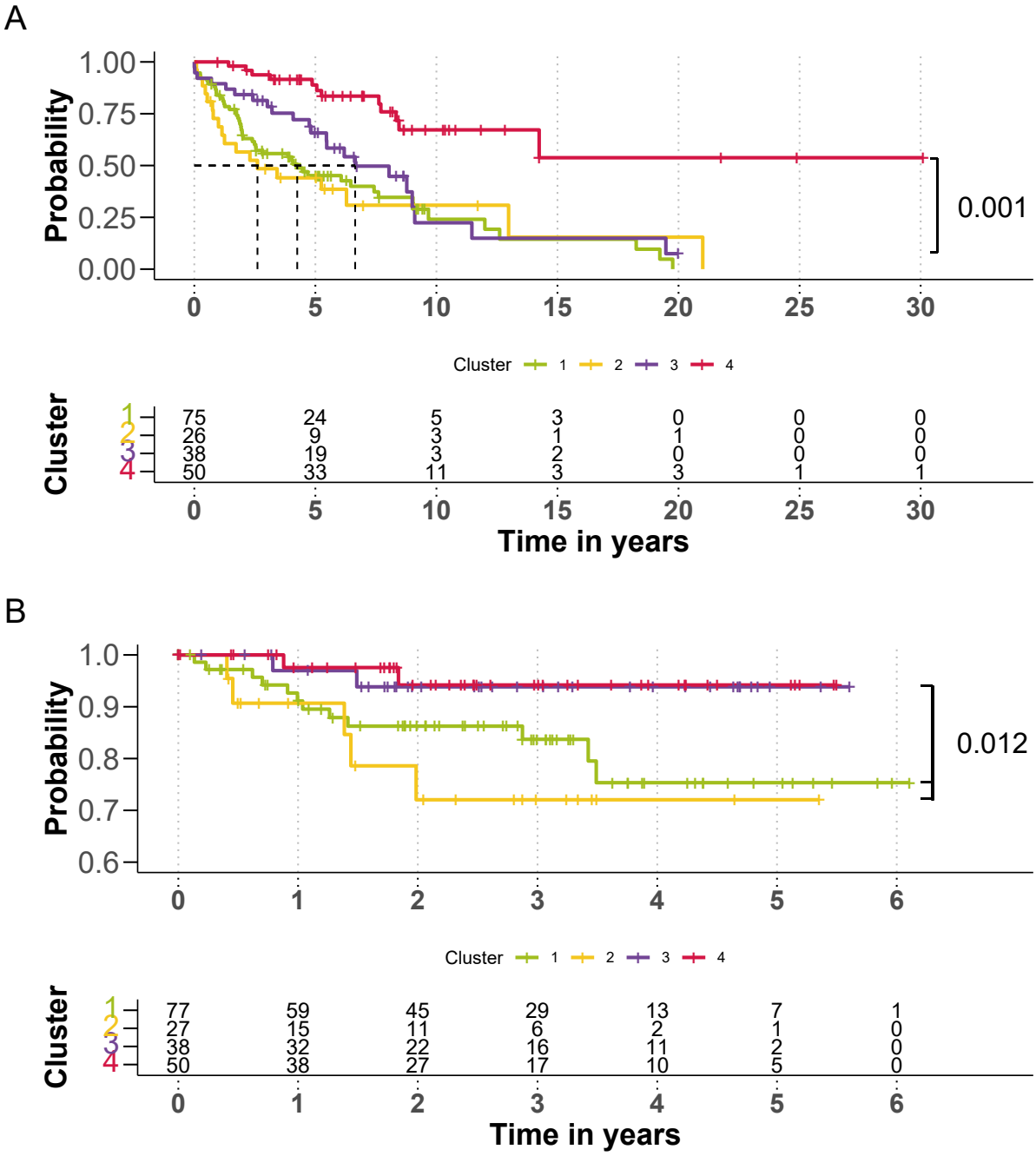

Appendix Figure 4. Time to first treatment and overall survival by clusters.

Kaplan-Meier curves of time to first treatment with p-value from univariate Cox proportional hazards model between C3 and C4 **(A)** and overall survival with p-value from univariate Cox proportional hazards model between C1&2 and C3&4 **(B)**. Median survival not reached.

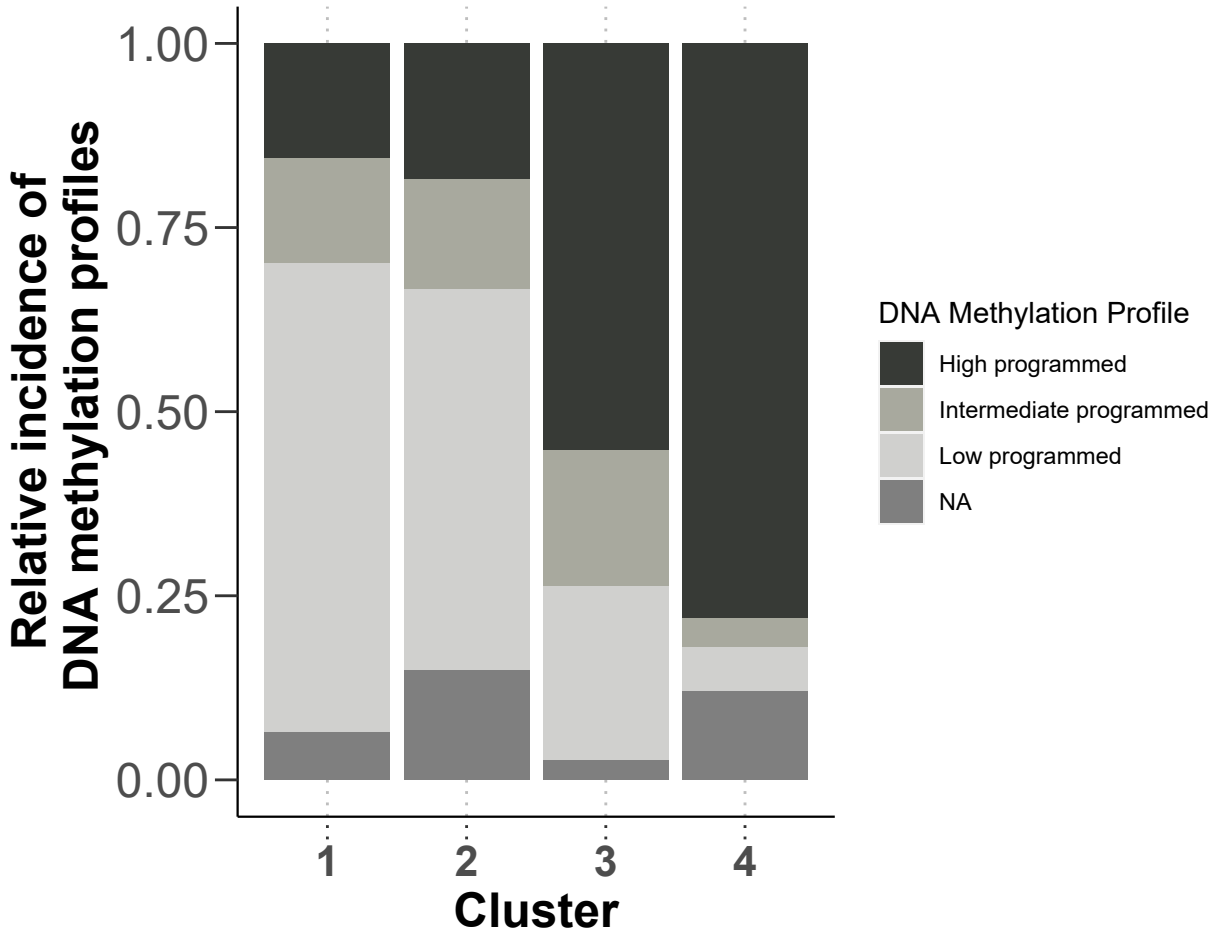

Appendix Figure 5. DNA Methylation profile of Clusters defined by response to microenvironmental stimuli

Barplot of DNA methylation profiles in the four clusters of microenvironmental response. C1 and C2 show higher abundance of low programmed (LP) DNA Methylation profiles, while C3 and C4 show more highly programmed (HP) DNA methylation clusters (C1: n=77; C2:n=27; C3: n=38; C4: n=50). NA=Not available.

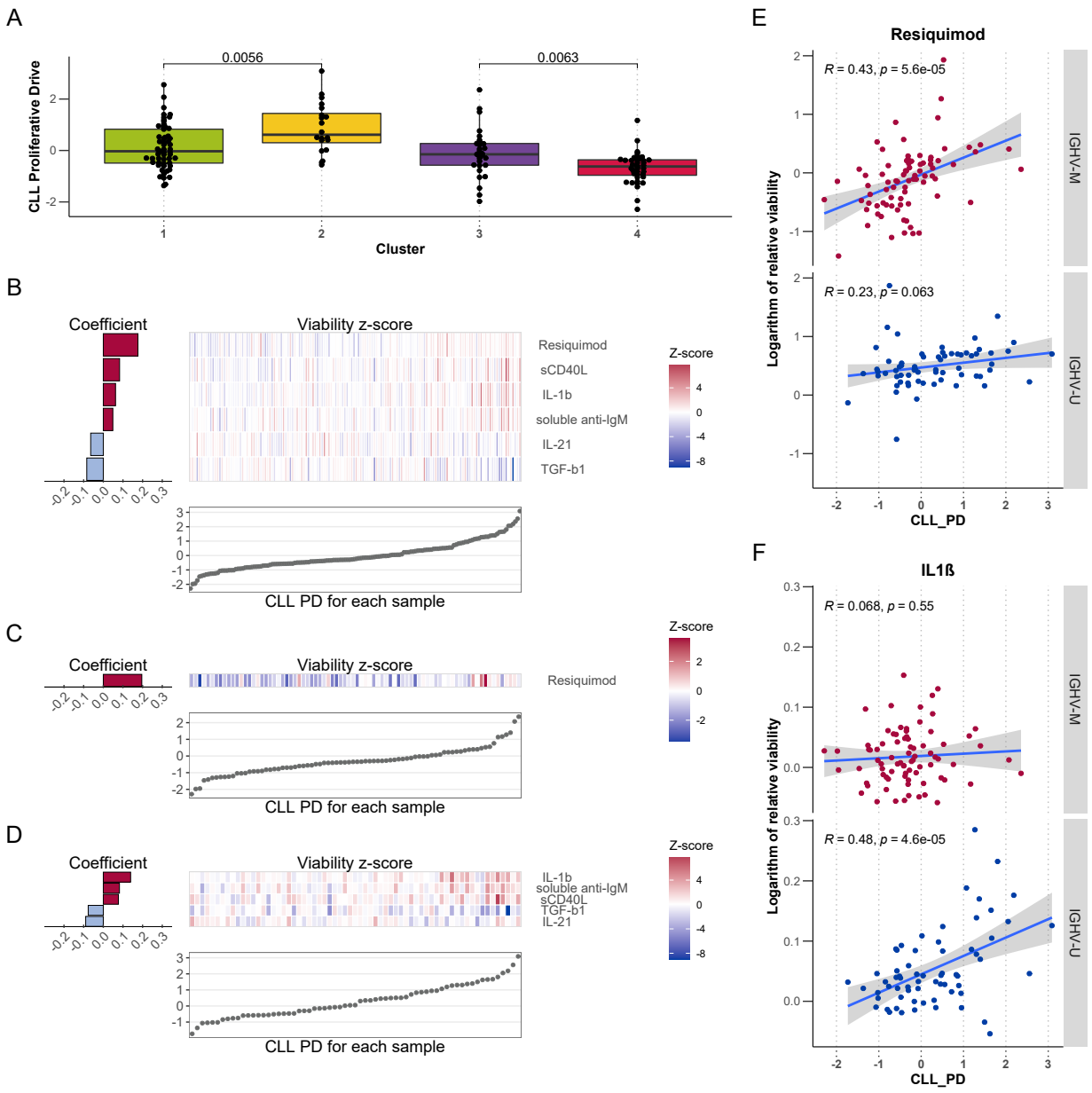

Appendix Figure 6. The relationship between CLL Proliferative Drive (as defined by Lu et al. (2021)[2]) and microenvironmental response.

(A) Beeswarm-boxplot of CLL-PD values stratified by cluster. P-values are from Student's t-tests (C1: n=57; C2:n=20; C3: n=29; C4: n=40). **(B-D)** Predictor profiles depicting relationship between CLL-PD and stimulus response. Stimuli that were associated to the size of CLL-PD were identified with Gaussian linear modelling with L1-penalty, using viability z-scores for each stimulus as feature matrix, and CLL-PD values as response matrix (n=146). Predictor profiles show z-scores of logarithm of relative viability for each stimuli associated with CLL-PD, bar plot on left shows size of coefficient assigned to each stimulus and scatter plot below indicates CLL-PD values for same patient sample. Coefficients are mean of 30 bootstrapped model fits, plotted when selected in >75% of fits. **(C)** shows model outputs for IGHV-M only samples (n=80) and **(D)** for IGHV-U only samples (n=65). **(E & F)** Exemplary scatter plots split by IGHV mutation status shown for Resiquimod **(E)** and IL1ß **(F)** (IGHV-M: n=80, IGHV-U: n=65). CLL-PD on x-axis and the logarithm of

relative viability after microenvironmental stimulation on y-axis. Pearson correlation coefficients are shown with p-values.

A

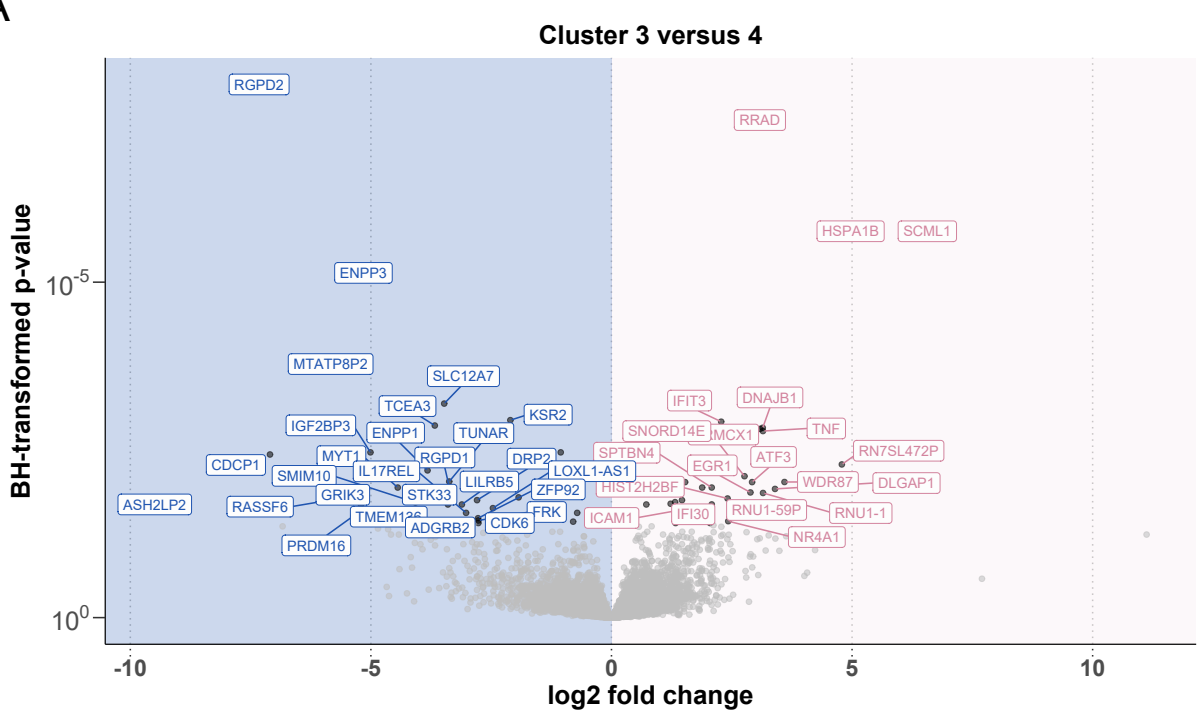
Cluster 3 versus 4
BH-transformed p-value
log2 fold change
RGPD2
RRAD
HSPA1B
SCML1
ENPP3
MTATP8P2
SLC12A7
TCEA3
KSR2
IGF2BP3
ENPP1
TUNAR
CDCP1
MYT1
RGPD1
DRP2
SMIM10
IL17REL
LOXL1-AS1
GRIK3
STK33
LILRB5
ZFP92
ASH2LP2
RASSF6
FRK
CDK6
ADGRB2
PRDM16
IFIT3
DNAJB1
SNORD14E
IMCX1
TNF
SPTBN4
EGR1
ATF3
RN7SL472P
WDR87
DLGAP1
HIST2H2BF
ICAM1
IFI30
RNU1-59P
RNU1-1
NR4A1

B

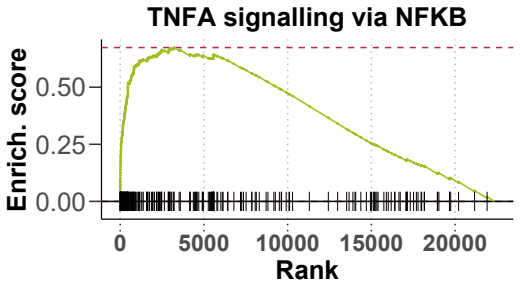
TNFA signalling via NFKB
Enrich. score
Rank

C

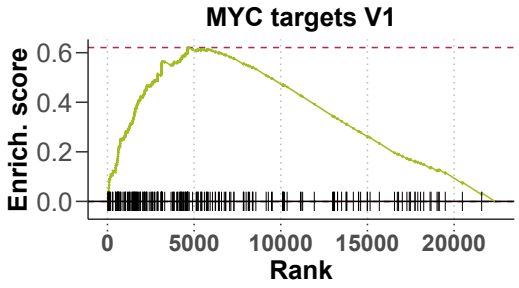
MYC targets V1
Enrich. score
Rank

D

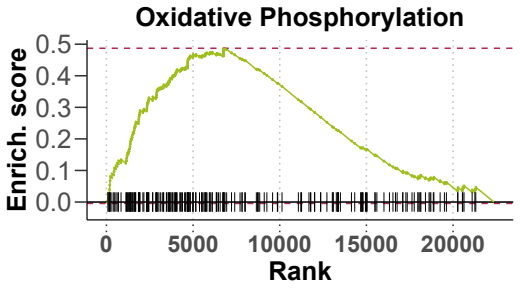
Oxidative Phosphorylation
Enrich. score
Rank

E

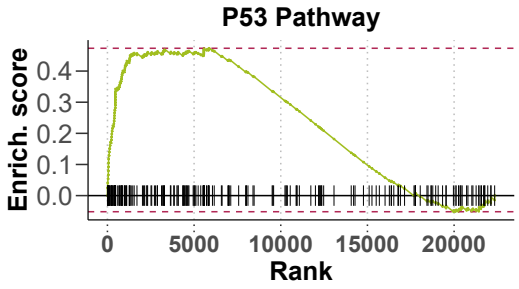
P53 Pathway
Enrich. score
Rank

Appendix Figure 7. RNA-Sequencing of matched samples indicates differential gene expression between Cluster 3 and Cluster 4.

Volcano plot of differentially expressed genes between Cluster 3 and Cluster 4 (C3: n=9; C4: n=12) **(A)**. X axis indicates log2 fold change values, calculated using the DESeq2 package, y axis gives corresponding -log10(transformed p-value). P-values transformed using BH method. Genes are labeled where p-value < 0.05. Enrichment plots of selected pathways **(B-D)**. Gene set enrichment analysis (GSEA) was performed with the Hallmark gene sets from the GSEA Molecular Signatures Database. Wald statistic was used to rank the genes. The green curve corresponds to the Enrichment Score curve, which is the running sum of the weighted enrichment score obtained from GSEA software.

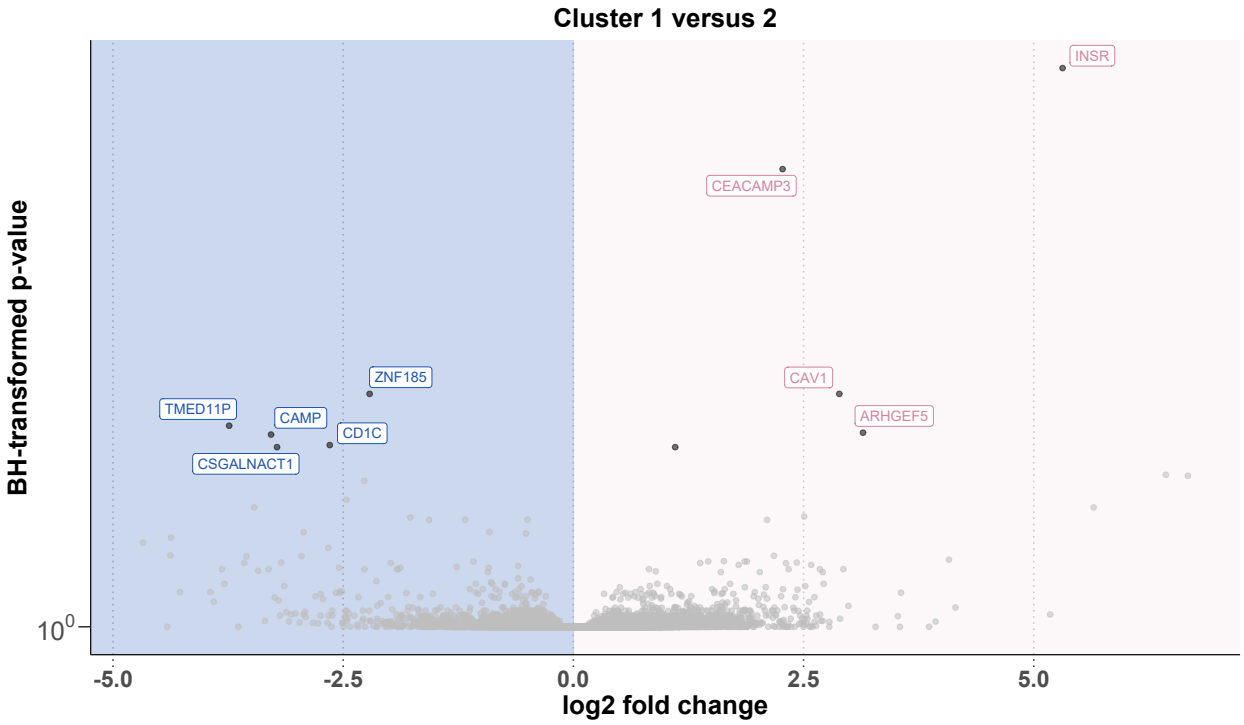

Appendix Figure 8. RNA-Sequencing of matched samples indicates differential gene expression between Cluster 1 and 2.

Volcano plot of differentially expressed genes between Cluster 1 and Cluster 2 (C1: n=17; C2: n=11). X axis indicates log2 fold change values, calculated using the DESeq package, y axis gives corresponding -log10(transformed p-value). P-values transformed using BH method. Genes are labeled where p-value<0.05.

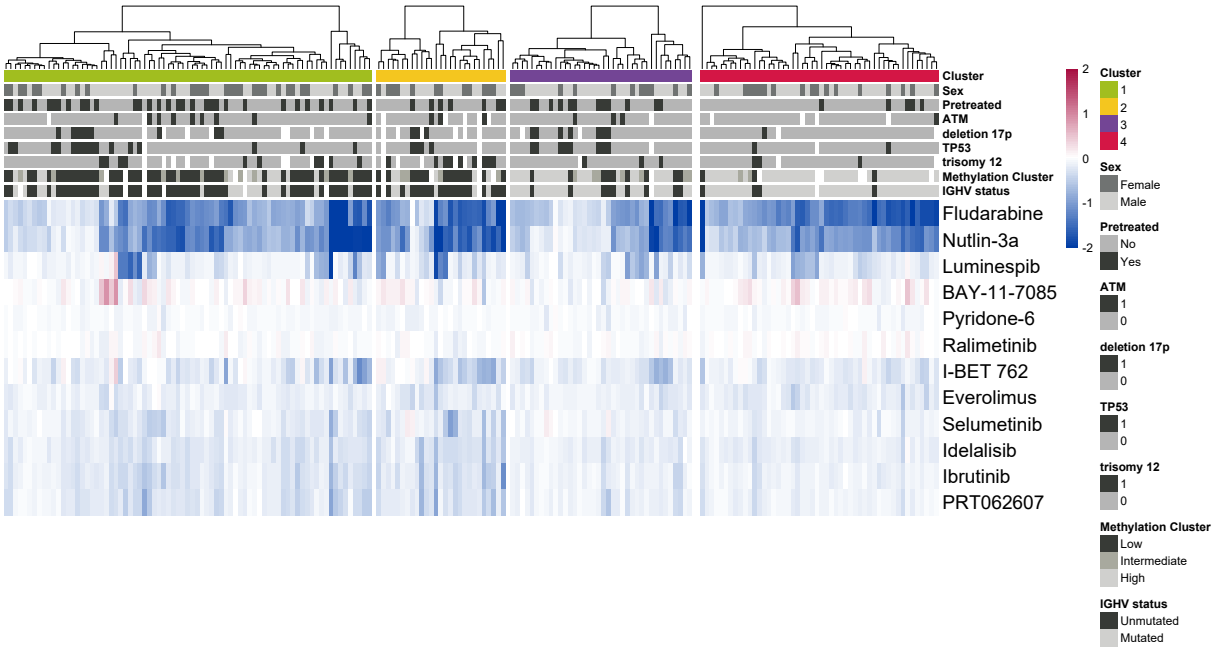

Appendix Figure 9. Drug response between clusters.

Heatmap showing the logarithm of relative viability after drug treatment. Rows represent drug treatments and columns represent primary CLL samples (n=192), annotated for their genetic background, sex and pretreatment status above. Red values indicate increased viability upon treatment, blue indicates decreased viability.

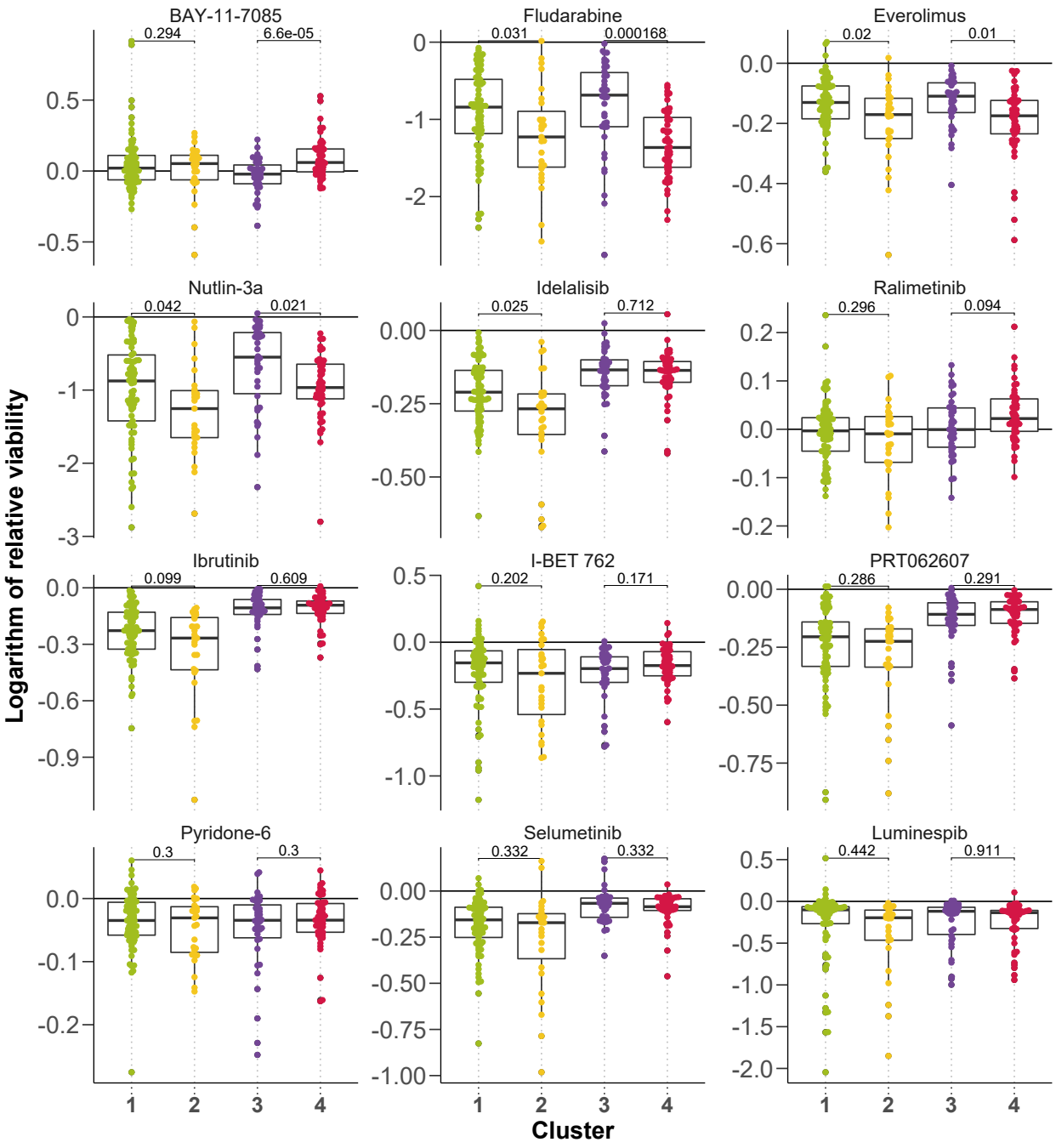

Appendix Figure 10. Drug response by clusters.

Logarithm of the relative viability after treatment with drugs, faceted by cluster. BH-transformed p-values from non-paired, two-sided Student's t-test are shown (C1: n=77; C2:n=27; C3: n=38; C4: n=50).

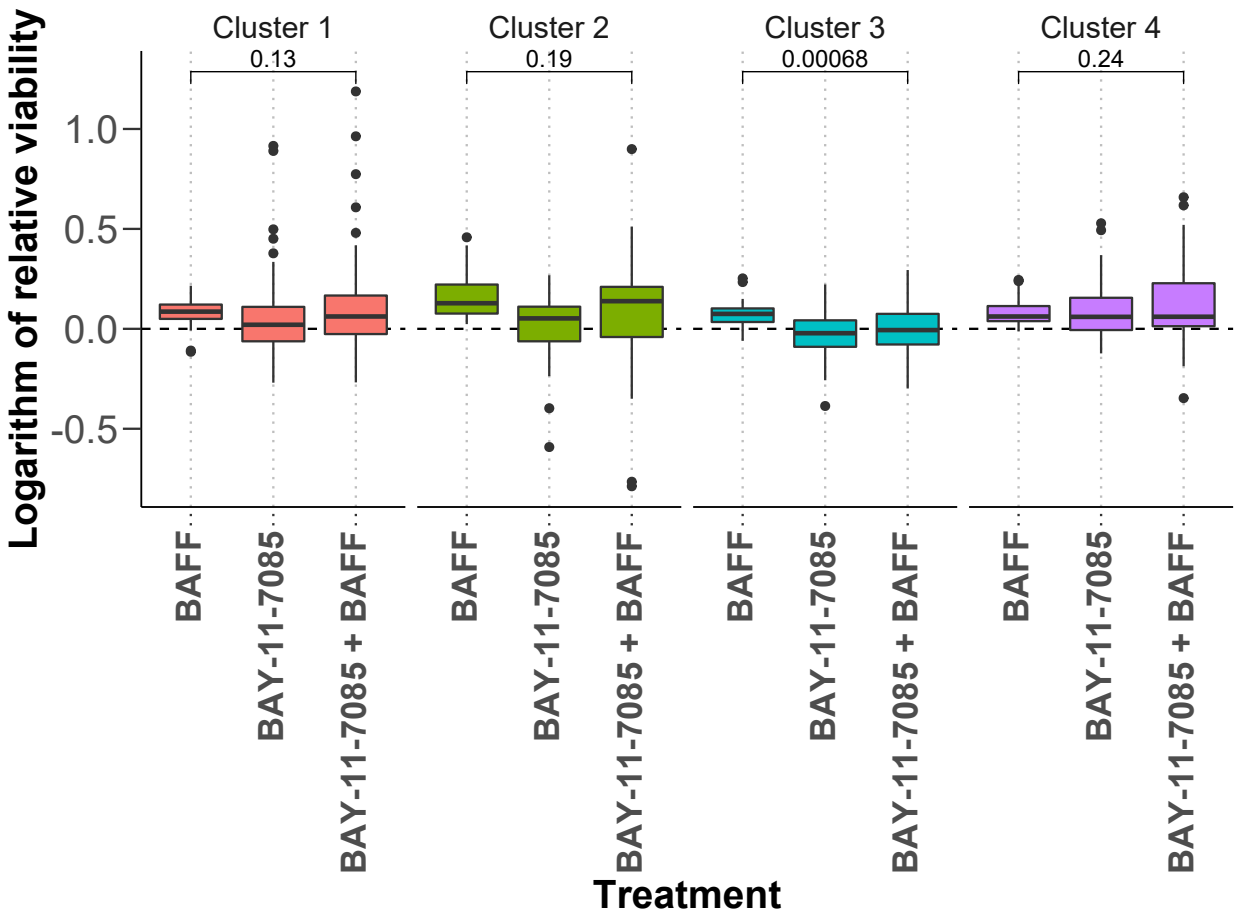

Appendix Figure 11. Effect of BAY-11-7085 treatment on BAFF response

Logarithm of the relative viability after treatment BAFF, BAY-11-7085 or both, faceted by cluster. P-values from paired, two-sided Student's t-test are shown (C1: n=77; C2:n=27; C3: n=38; C4: n=50).

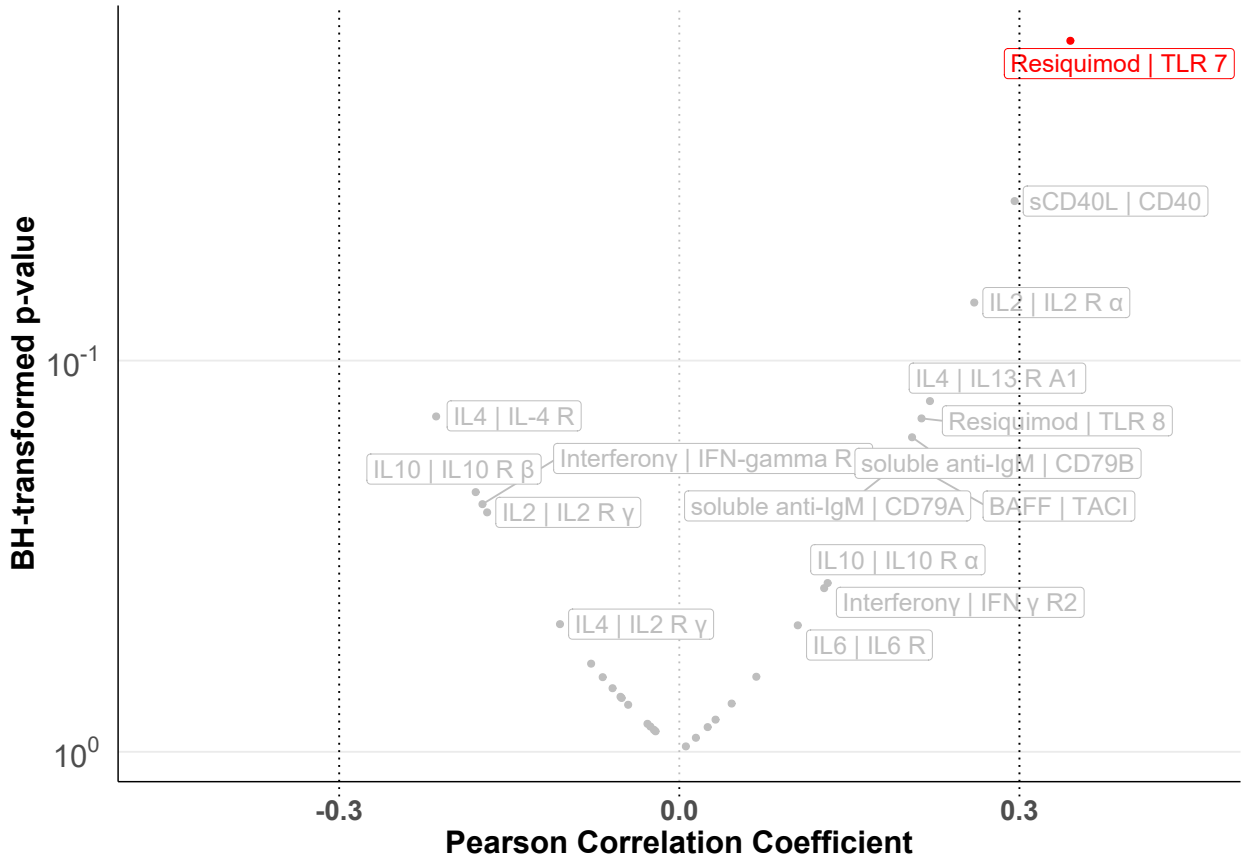

Appendix Figure 12. Correlation of stimulus response and receptor expression.

Volcano plot depicts Pearson correlation coefficients against corresponding BH-transformed p-values, for the correlation between the logarithm of the relative viability and vst RNA counts of corresponding stimulus receptor (n=49). RNA counts taken from RNA-Sequencing of untreated matched CLL patient sample. Only viability after treatment with Resiquimod correlated with receptor expression (R>0.3).

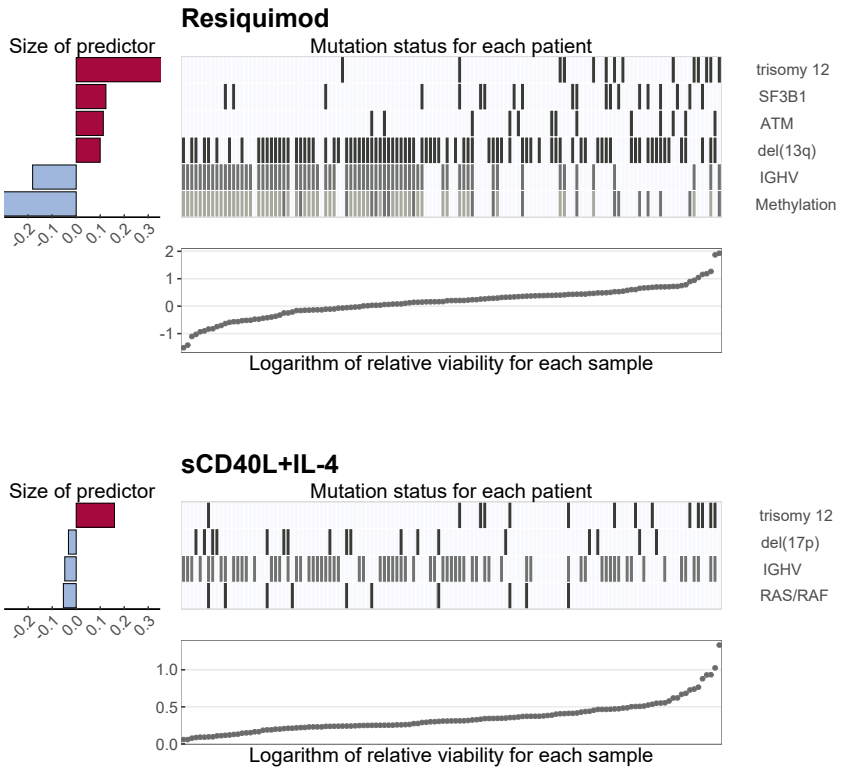

Appendix Figure 13. Predictor profiles to represent genetic feature-stimulus associations.

Stimuli which are not shown in Figure 3B but have predictors >0.02 assigned by multivariate analysis using Gaussian linear modelling with L1-penalty are shown. Within the plots, the bar plots on left indicate size and sign of coefficients assigned to the named predictors. Positive coefficients indicate higher viability after stimulation if the feature is present. Scatter plots indicate the logarithm of relative viability values, in order of magnitude, for each individual sample. Heatmaps show status for each of the genetic predictors for corresponding sample in scatter plot (n=128).

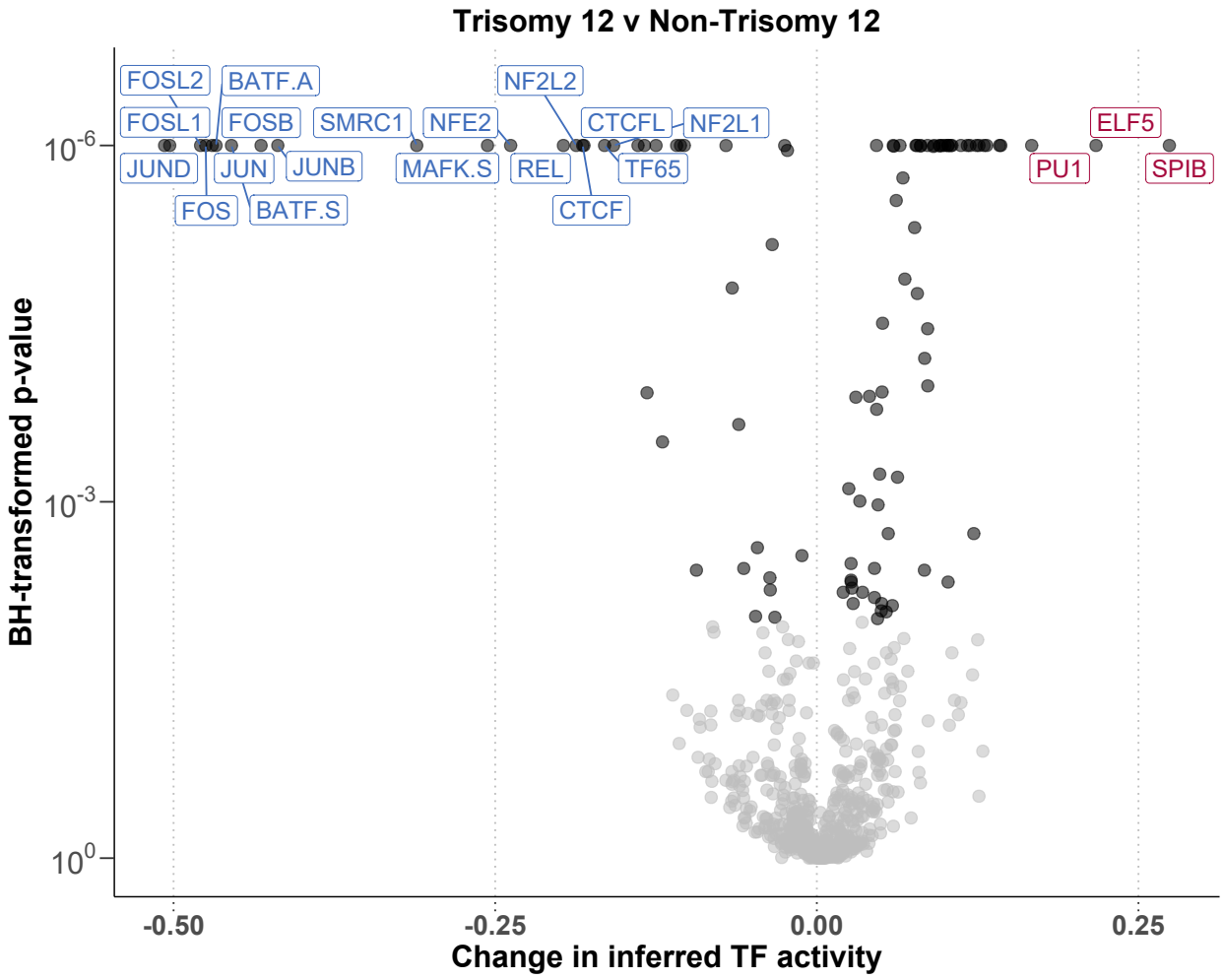

Appendix Figure 14. ATACseq comparing trisomy 12 and non-trisomy 12 CLL samples.

Volcano plot shows change in inferred TF activity (x-axis) against transformed p-values (y-axis) for trisomy 12 (n = 2) versus non-trisomy 12 samples (n = 2). Inferred TF activity calculated using the diffTF package, TFs are labeled where inferred activity > 0.15, and BH-transformed p-value < 0.01.

```
## <ScaleContinuousPosition>
##  Range:
##  Limits:    0 --    1
```

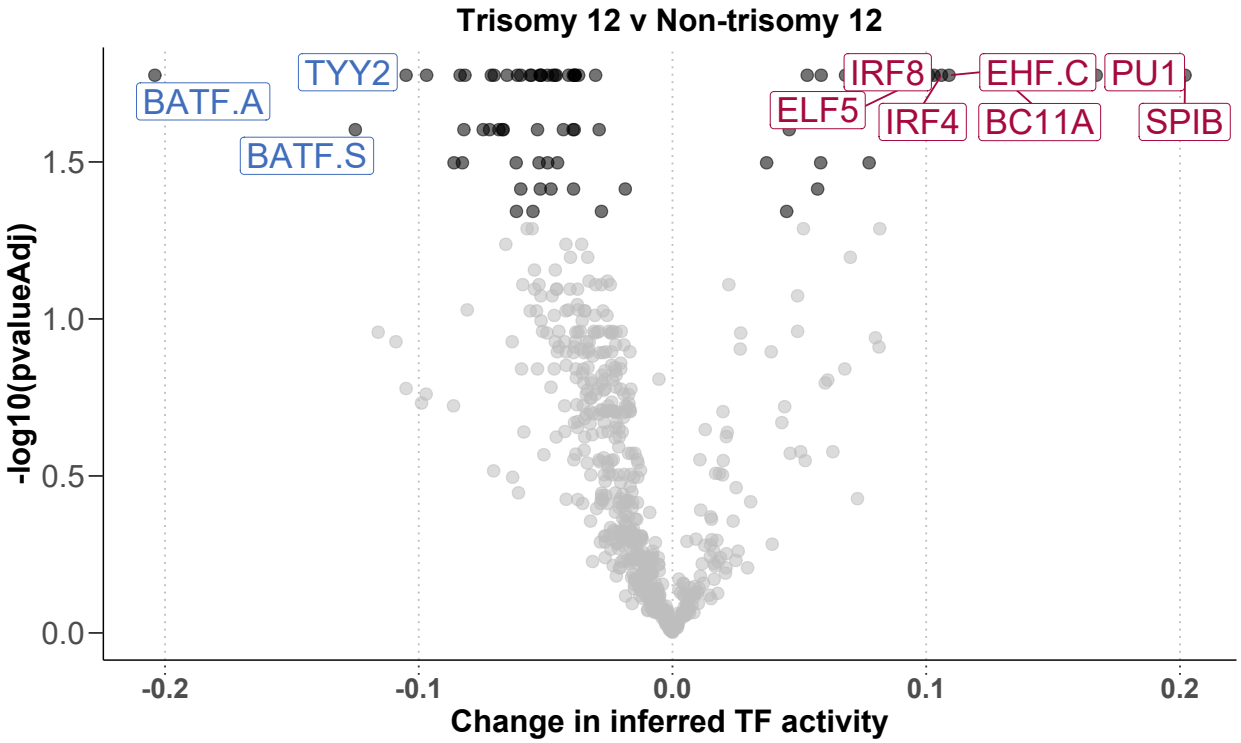

Appendix Figure 15. ATACseq comparing trisomy 12 and non-trisomy 12 CLL samples.

Volcano plot shows change in inferred TF activity (x-axis) against transformed p-values (y-axis) for trisomy 12 (n = 13) versus non-trisomy 12 samples (n = 87). Inferred TF activity calculated using the diffTF package, and measured as weighted mean difference. p-values are obtained through diffTF in permutation mode and transformed by the Benjamini-Hochberg procedure. TFs are labeled where absolute weighted mean difference > 0.1, and transformed p-value < 0.05. Data from Beekman et al. 2018[4].

A

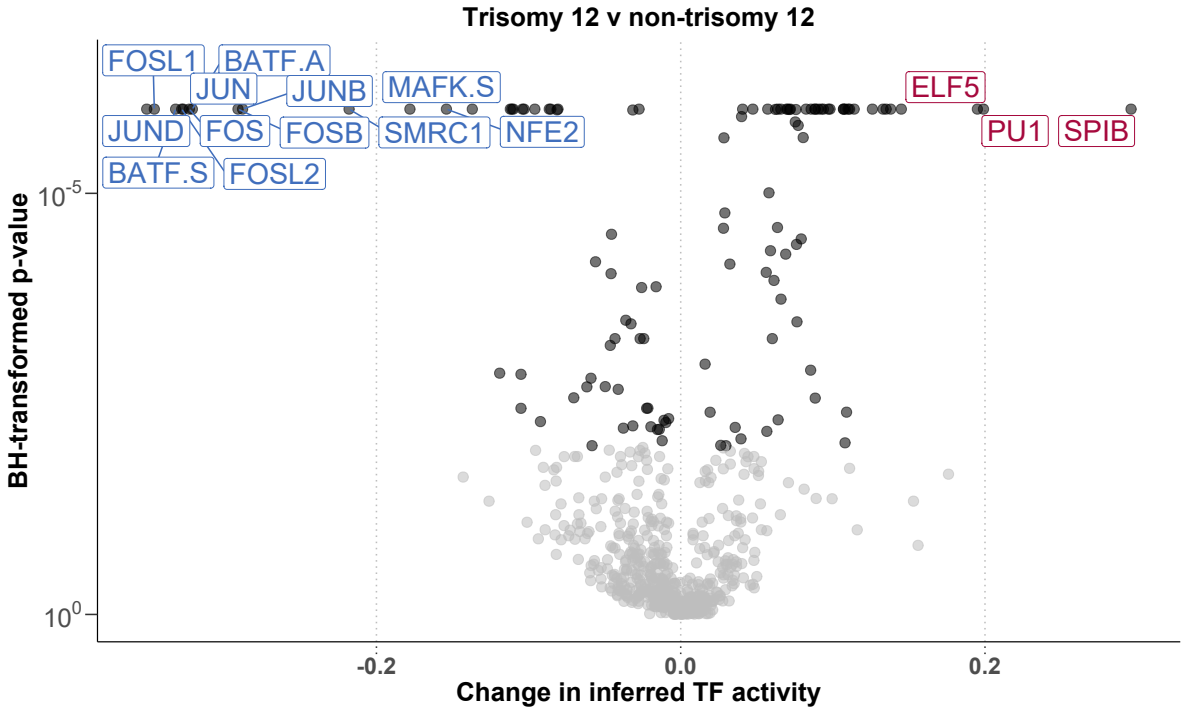
Trisomy 12 v non-trisomy 12
FOSL1
BATF.A
JUN
JUNB
MAFK.S
ELF5
JUND
FOS
FOSB
SMRC1
NFE2
PU1
SPIB
BATF.S
FOSL2
10^{-5}
10^{0}
BH-transformed p-value
-0.2
0.0
0.2
Change in inferred TF activity

B

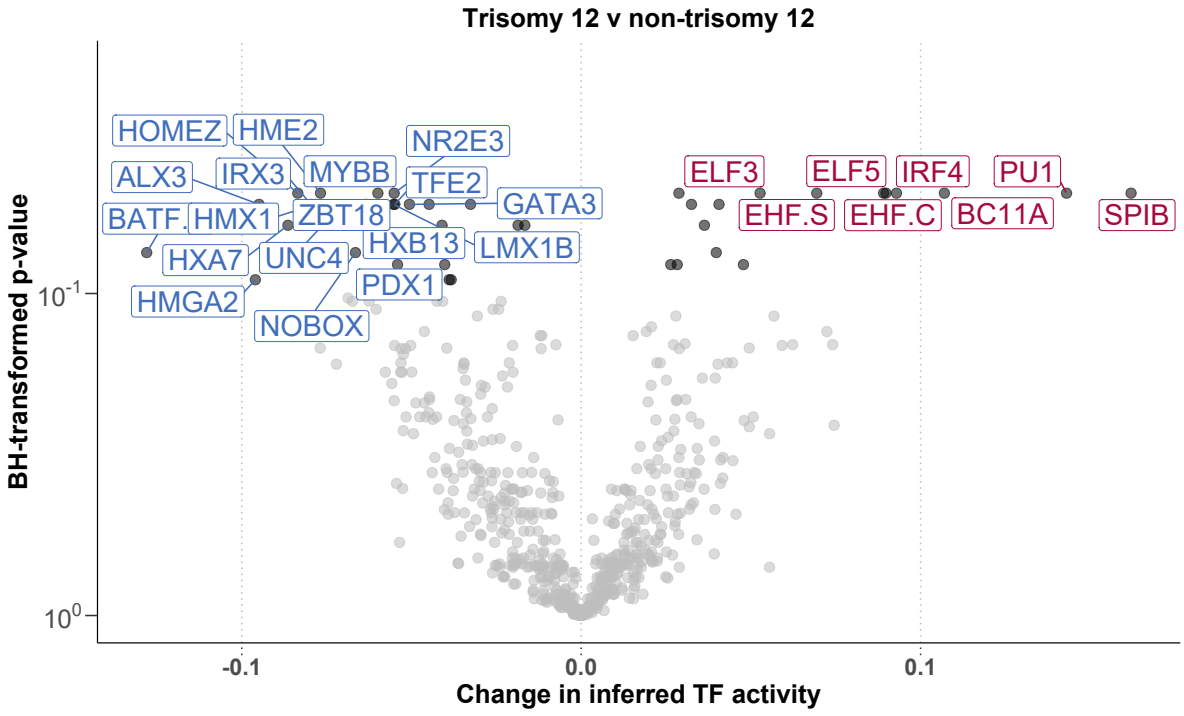
Trisomy 12 v non-trisomy 12
HOMEZ
HME2
NR2E3
ALX3
IRX3
MYBB
TFE2
ELF3
ELF5
IRF4
PU1
GATA3
BATF.
HMX1
ZBT18
EHF.S
EHF.C
BC11A
SPIB
HXB13
LMX1B
HXA7
UNC4
PDX1
HMGA2
NOBOX
10^{-1}
10^{0}
BH-transformed p-value
-0.1
0.0
0.1
Change in inferred TF activity

Appendix Figure 16. ATACseq comparing trisomy 12 and non-trisomy 12 CLL samples, independent of third copy of chromosome 12

Volcano plot shows change in inferred TF activity (x axis) against transformed p-values (y axis) for trisomy 12 versus non-trisomy 12 samples, for (A) the 2 versus 2 comparison and (B) the 9 versus 42 comparison based on the data from Rendeiro et al. 2016[3]. Input peak files supplied to diffTF did not include peaks on chromosome 12. p-values are obtained through diffTF in (A) analytic mode and (B) permutation mode, transformed by the Benjamini-Hochberg procedure. TFs are labelled in (A) where absolute weighted mean difference > 0.15, and transformed p-value < 0.01 and in (B) where absolute weighted mean difference > 0.05, and transformed p-value < 0.1.

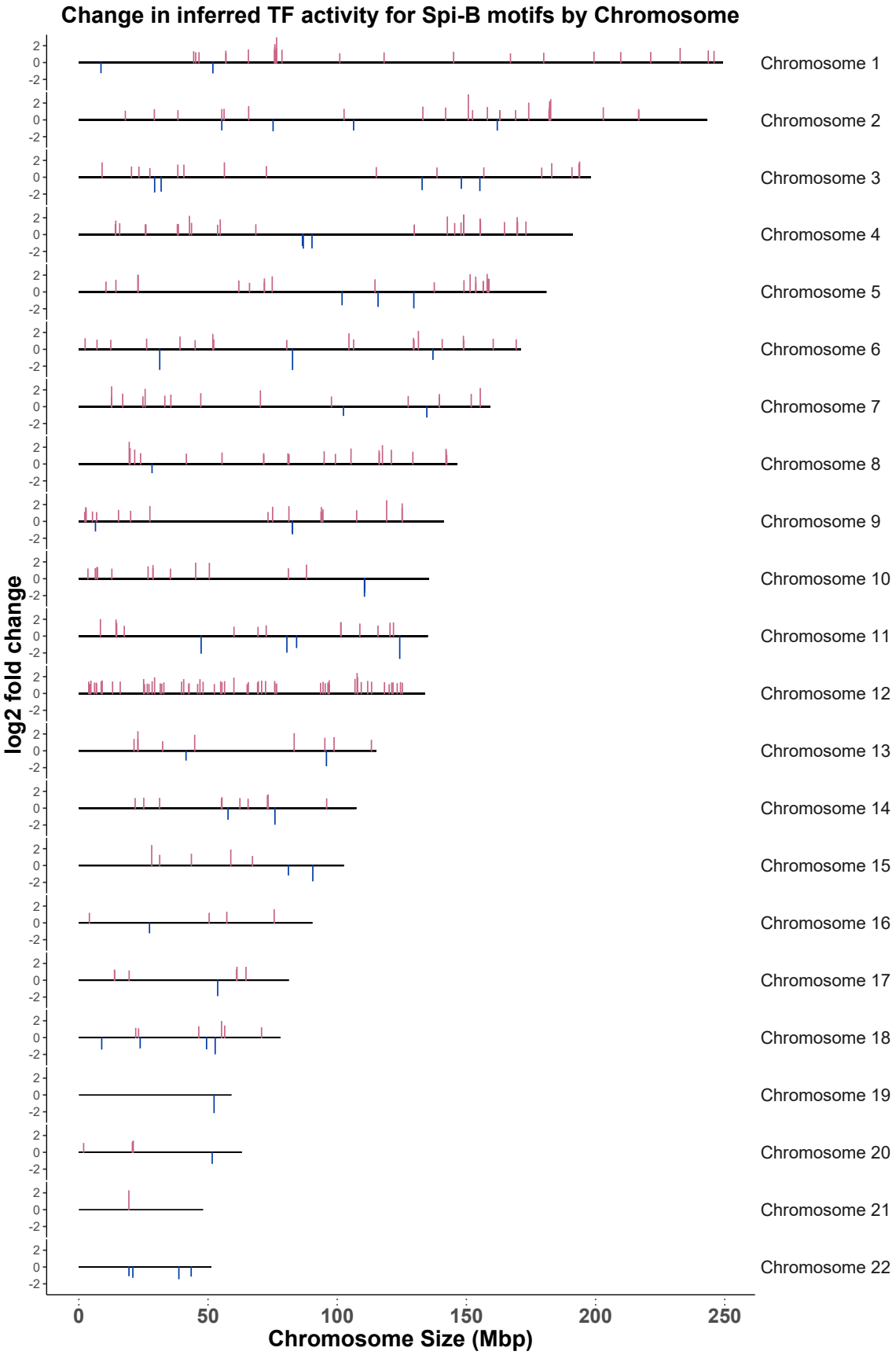
Change in inferred TF activity for Spi-B motifs by Chromosome
log2 fold change
2
0
-2
Chromosome 1
Chromosome 2
Chromosome 3
Chromosome 4
Chromosome 5
Chromosome 6
Chromosome 7
Chromosome 8
Chromosome 9
Chromosome 10
Chromosome 11
Chromosome 12
Chromosome 13
Chromosome 14
Chromosome 15
Chromosome 16
Chromosome 17
Chromosome 18
Chromosome 19
Chromosome 20
Chromosome 21
Chromosome 22
0
50
100
150
200
250
Chromosome Size (Mbp)

Appendix Figure 17. Chromosomal locations of Spi-B motifs that show differential accessibility between trisomy 12 and non-trisomy 12 CLL.

Log2 fold changes are plotted (y axis) for Spi-B motifs that show an absolute Log2 fold change > 1 and a p-value < 0.1, as calculated using the diffTF package for all Spi-B motif locations, (motif defined in the HOCOMOCO database). Data shown is the 9 (trisomy 12 CLL) versus 42 (non-trisomy 12 CLL) comparison based on the data from Rendeiro et al. 2016[3].

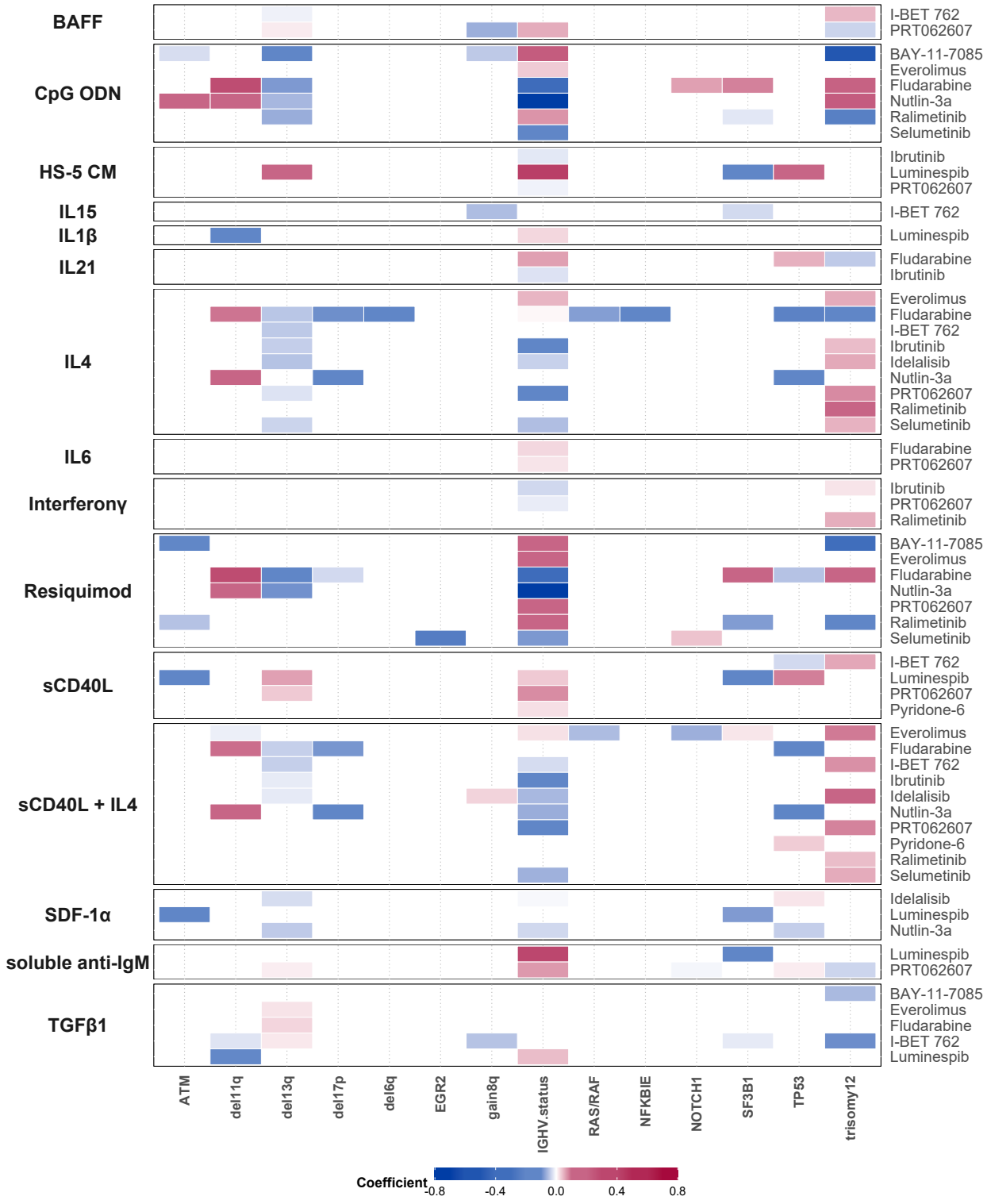

Appendix Figure 18. Genetic predictors of drug-stimulus interactions.

Based on the drug-stimulus viability data of 137 CLL patient samples with complete genetic annotation, we fitted a sample specific linear model. Heatmap depicting overview of genetic predictors of drug - stimulus interactions (each row represents the coefficients from fitting a single multivariate model). Stimuli are shown

on left, and corresponding drugs on right. Drugs, stimuli and genetic alterations are alphabetically sorted. Coloured fields indicate that the interaction coefficient for given drug and stimulus is modulated by corresponding genetic feature. Positive coefficients are shown in red, indicating the interaction coefficient is more positive for given drug and stimulus combination if the feature is present.

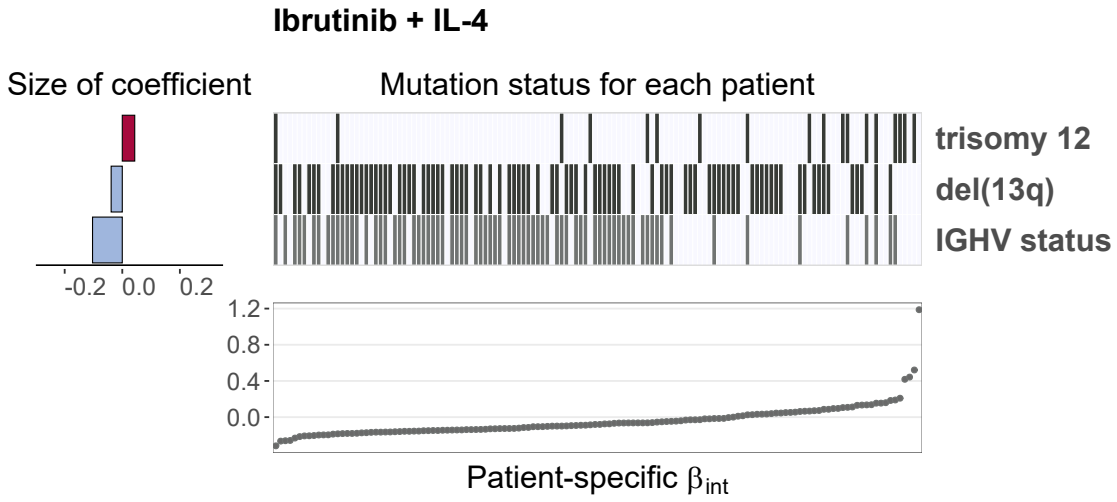

Appendix Figure 19. Genetic predictors of the interaction between ibrutinib and IL4.

Predictor profile depicting genetic features that modulate the size of the β_{int} for ibrutinib and IL4. To generate the predictor profile, linear model in Equation 1 was fitted in a sample-specific manner, to calculate drug-stimulus β_{int} s for each patient sample (n=137). Ranked patient-specific β_{int} values are shown in lower scatter plot. Associations between the size of the β_{int} and genetic features were identified using multivariate regression with L1 (lasso) regularisation, with gene mutations and IGHV status as features, and selecting coefficients that were chosen in >90% of bootstrapped model fits. The horizontal bars on left show the size of fitted coefficients assigned to genetic features. Matrix above scatter plot indicates patient mutation status for the selected genetic features. Matrix fields correspond to points in scatter plot (i.e. patient data is aligned), to indicate how the size of the β_{int} varies with selected genetic feature.

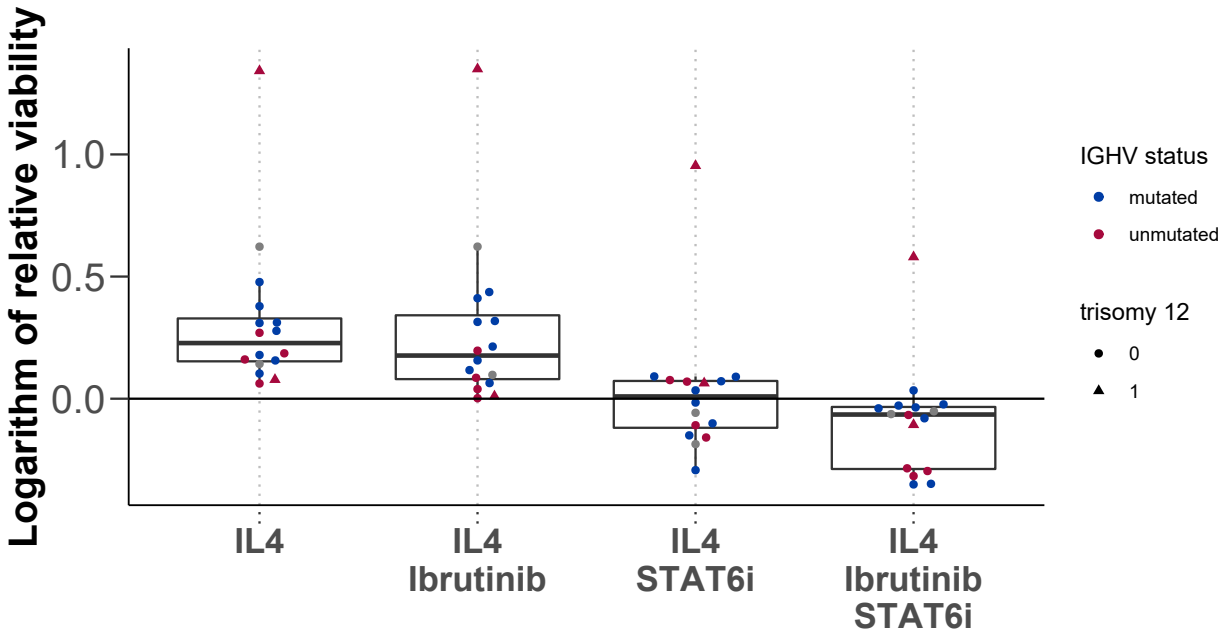

Appendix Figure 20. STAT6 dependency of IL4 signaling.

Natural logarithm of the relative viability after treatment with IL4 in combination with ibrutinib, the STAT6 inhibitor AS1517499, and both (n=16). The effects observed with IL4 stimulation are dependent on STAT6 activation. Addition of the STAT6 inhibitor AS1517499 could revoke the effect on baseline viability as well as drug induced toxicity.

References

1. Care, M.A., Cocco, M., Laye, J.P., et al. (2014) SPIB and BATF provide alternate determinants of IRF4 occupancy in diffuse large B-cell lymphoma linked to disease heterogeneity. Nucleic Acids Res 42: 7591–7610
2. Lu, J., Cannizzaro, E., Meier-Abt, F. et al. Multi-omics reveals clinically relevant proliferative drive associated with mTOR-MYC-OXPHOS activity in chronic lymphocytic leukemia. Nat Cancer 2, 853–864 (2021).
3. Rendeiro, A., Schmidl, C., Strefford, J. et al. Chromatin accessibility maps of chronic lymphocytic leukaemia identify subtype-specific epigenome signatures and transcription regulatory networks. Nat Commun 7, 11938 (2016).
4. Beekman, R., Chapaprieta, V., Russiñol, N. et al. The reference epigenome and regulatory chromatin landscape of chronic lymphocytic leukemia. Nat Med 24, 868–880 (2018).